Precise aftershock distribution of the 2005 West Off Fukuoka Prefecture Earthquake (Mj=7.0) using a dense onshore and offshore seismic network

Kenji Uehira[1], Tomoaki Yamada[2], Masanao Shinohara[2], Kazuo Nakahigashi[2], Hiroki Miyamachi[3], Yoshihisa Iio[4], Tomomi Okada[5], Hiroaki Takahashi[6], Norimichi Matsuwo[1], Kazunari Uchida[1], Toshihiko Kanazawa[2], and Hiroshi Shimizu[1]

[1]*Institute of Seismology and Volcanology, Kyushu University, Shimabara 855-0843, Japan*
[2]*Earthquake Research Institute, University of Tokyo, Tokyo 113-0032, Japan*
[3]*Faculty of Science, Kagoshima University, Kagoshima 890-0065, Japan*
[4]*Disaster Prevention Research Institute, Kyoto University, Uji 611-0011, Japan*
[5]*Graduate School of Science, Tohoku University, Sendai 980-8578 Japan*
[6]*Institute of Seismology and Volcanology, Hokkaido University, Sapporo 060-0810, Japan*

(Received December 7, 2005; Revised July 25, 2006; Accepted August 1, 2006; Online published February 2, 2007)

The 2005 West Off Fukuoka Prefecture Earthquake (Mj=7.0) occurred on March 20, 2005 in the northern part of Kyushu, Japan. To study the aftershock activity, we deployed eleven pop-up type ocean bottom seismometers (OBSs), sixteen locally recorded temporary stations, and eight telemetered temporary stations in and around the epicenter region. We combined data from these stations and permanent stations located around the aftershock area, and determined the hypocenter of the mainshock and aftershocks. The mainshock was in the northwestern central part of the aftershock region, at a depth of 9.5 km. The mainshock was on a left-lateral strike-slip fault. Aftershocks were located in a depth range of 1–16 km and laterally extend for about 25 km in a NW-SE direction. We found that the aftershocks fell into four groups. This might be due to the heterogeneous structure in the source region. In the group that includes the mainshock, we estimated two fault planes bordering on the depth of the mainshock. There are 10-degree differences in both strike and dip angles between the lower and upper planes. From the aftershock distribution and the focal mechanisms, the rupture first propagated downward, and then propagated upward.

Key words: The 2005 West Off Fukuoka Prefecture Earthquake, aftershock distribution, ocean bottom seismometer (OBS), temporary telemetered and locally recorded observations.

1. Introduction

The 2005 West Off Fukuoka Prefecture Earthquake occurred in Genkai-nada, Fukuoka Prefecture, in the northern part of Kyushu, Japan, at 10:53 on March 20, 2005 (JST) with a Japan Meteorological Agency (JMA) magnitude (Mj) of 7.0. According to JMA, a maximum intensity of 6− on the JMA scale was observed in Fukuoka City, in Maebaru City, and in the Saga Prefecture town of Miyaki. This earthquake killed one person and injured more than 1,000 people. Many aftershocks occurred following the mainshock, the largest was magnitude Mj=5.8 at 06:11 on April 20, 2005 (JST).

In the northern part of Kyushu there are many active faults such as the Kego fault and the Nishiyama fault (The Research Group for Active Faults of Japan, 1991), and this fact indicates that earthquakes greater than M7 have occurred during the last few tens of thousands of years. However, seismic activity in this area has been very low throughout recorded history. In fact, only three earthquakes of M>5 have occurred during recorded history, the largest being a magnitude M=6.0 on August 10, 1898, and seismic activity observed by the recently developed seismic network has also been very low. Moreover, low strain rates were found in this area by GPS data analysis (Sagiya *et al*., 2000) and a triangulation survey (Geographical Survey Institute, 1987). From these facts, Uehira and Shimizu (2005) stated that there was almost no possibility of a large earthquake occurring in the near-future.

After the mainshock, various surveys, such as GPS observation (Nakao *et al*., 2006), dense seismic array observation (Matsumoto, S. *et al*., 2006), and so on, were carried out. We deployed temporary seismic stations just above the aftershock area (Shimizu *et al*., 2006) in order to constrain the focal depths, mechanisms of aftershocks, shear wave polarization anisotropy (Watanabe *et al*., 2006), and spatial distribution of static stress drops (Iio *et al*., 2006). We combined data from both the temporary stations and permanent stations around the aftershock area, and relocated aftershocks using a joint hypocenter determination (JHD) technique. To explain travel-time data, one model is based on a 3D velocity structure and hypocentral distribution (Hori *et al*., 2006), and another is based on a 1D velocity structure, station correction values, and hypocentral distribution. These two models are different in the number of model parameters. Generally speaking, a smaller number of model parameters gives more stable results. Therefore we chose a

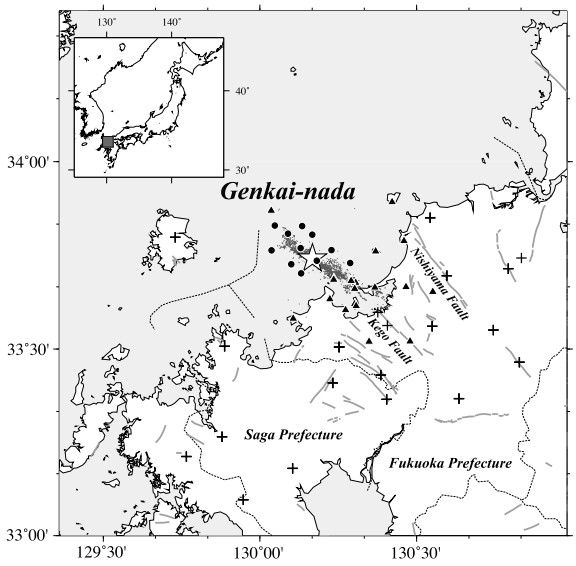

Fig. 1. Map showing the location of the stations (cross: permanent telemetered, triangle: temporary telemetered or locally recorded, circle: OBS) used in this study. The star denotes the epicenter of the mainshock and gray dots denote the aftershocks to be relocated in this study. The dashed lines indicate prefecture borders. Bold gray lines indicate the active faults (The Research Group for Active Faults of Japan, 1991). In the insert map, the target area is shown with respect to greater parts of Japan Islands by the dark gray rectangle.

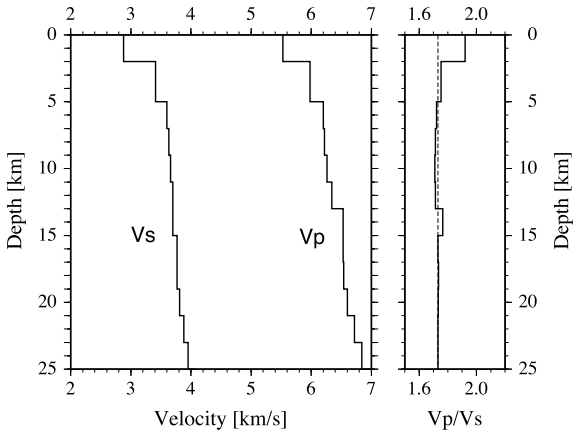

Fig. 2. One-dimensional velocity models of the *P*- and *S*- waves from 0 to 25 km depth. The Vp/Vs is also shown on the right side. The solid lines denote the velocity models obtained from the JHD relocation.

simple model (i.e. 1D velocity structure, station correction values, and hypocentral distribution) and discuss the range in which this model is valid. This study aims to determine the precise aftershock distribution (especially depth) and the focal mechanisms, and to discuss the source process of the earthquake using the improved aftershock distribution.

2. Data and Hypocenter Determination

We used waveform data from 11 pop-up type OBSs, 16 locally recorded temporary stations, eight telemetered temporary stations (Shimizu *et al.*, 2006), and 20 permanent stations installed by the city of Fukuoka, JMA, the National Research Institute for Earth Science and Disaster Prevention (NIED), and the Institute of Seismology and Volcanology, Kyushu University (SEVO) (Fig. 1). *P* and *S* arrival

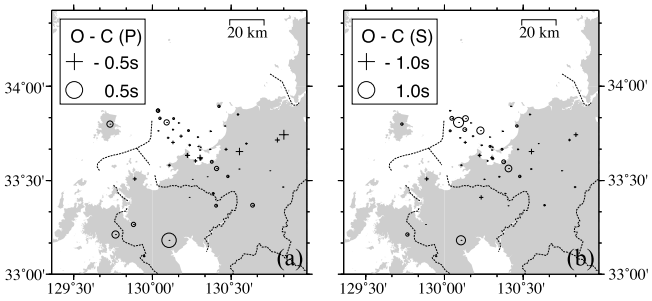

Fig. 3. Travel-time corrections for the *P*- and *S*-waves derived from the JHD relocation. (a) for the *P*-waves and (b) for the *S*-waves. The circles indicate the positive residuals, while the crosses denote the negative residuals. Reference sizes are shown in the insets.

times were identified on a computer display (Urabe and Tsukada, 1991).

Since the number of seismic stations changed with time (Shimizu *et al.*, 2006), it is possible that systematic errors of hypocenter locations may have arisen. We therefore calculated 1D velocity models and station correction values using data from the time given by the most dense network, and applied these values to data of other periods.

We selected 301 master events using the following criteria: (1) occurrence from March 26 to April 14, 2005, because we had the most dense seismic network during this period (i.e. the OBSs were installed), (2) the total number of *P*- and *S*-arrival times greater than or equal to 30 and 20, respectively, and (3) the number of *P*- and *S*-arrival times at the permanent stations greater than or equal to 18 and 5, respectively. Then we determined simultaneously the hypocentral parameters, the 1D velocity models of *P*- and *S*-waves (Fig. 2) and the travel-time corrections for the *P*- and *S*- waves for the 54 stations (Fig. 3) using the JHD technique (Kissling *et al.*, 1994). *Vp* and *Vs* are well resolved down to 17 km. After the JHD procedure, the root-mean-square (RMS) of the travel time residuals decreased to 0.088 s.

We applied these 1D velocity models and the station correction values to data from other periods. Hypocenters were relocated by the maximum-likelihood estimation technique of Hirata and Matsu'ura (1987), and the magnitudes of the aftershocks were estimated using the maximum amplitude of the seismic record (Watanabe, 1971). Finally, we selected 2,503 events using the following criteria: (1) occurrence from March 20 to May 31, 2005, (2) magnitude greater than or equal to 1.5, (3) the number of *P*- and *S*-arrival times greater than or equal to 16 and 8, respectively, and (4) errors smaller than 0.6 km in EW, 0.6 km in NS, and 1.6 km in depth. We found that the errors were smaller than 0.25 km in EW, 0.25 km in NS, and 0.7 km in depth for more than 90% of the 2,503 relocated events.

3. Results

3.1 Comparison of hypocenter distribution detected by different seismic networks

Figure 4(a) shows a comparison of hypocenters detected by all the seismic stations (gray circles) and those detected only by permanent stations (orange circles), and Fig. 4(b) compares hypocenters detected by all seismic stations (gray circles) and those detected by all but OBS stations (red cir-

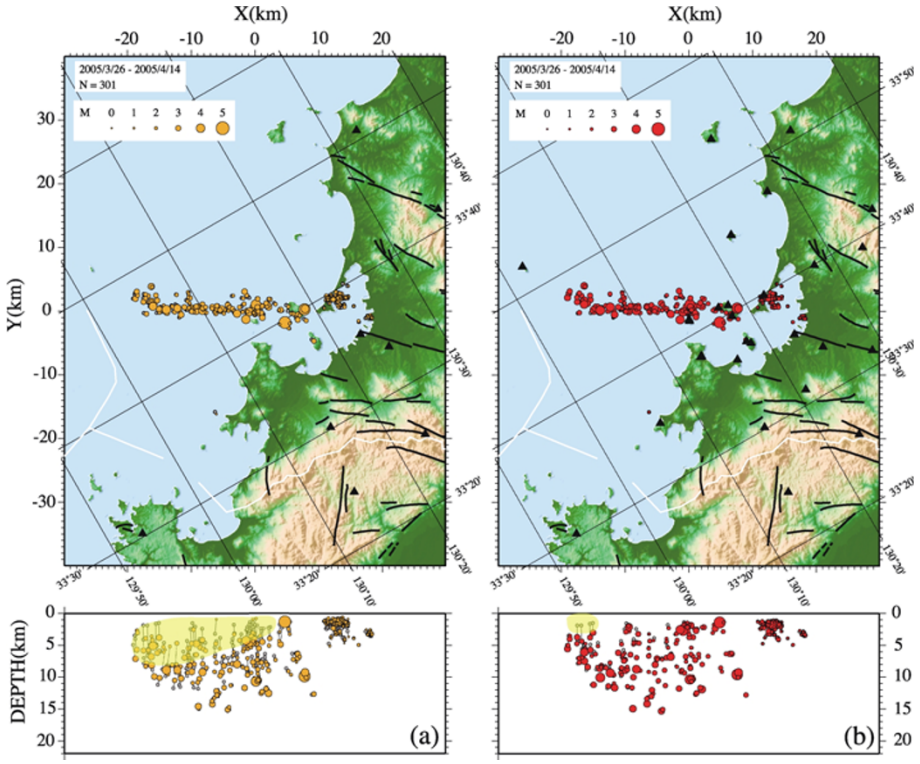

Fig. 4. Differences in the relocated hypocenter positions by station distribution. Note that the map is rotated counterclockwise by 30 degrees, so that the X-axis is parallel to the aftershock distribution. We show X-Y cross-sections (upper) and X-DEPTH cross-sections (lower). (a) Comparison of hypocenters located by all seismic stations (gray circles) and those by only permanent stations (orange circles). (b) Comparison of hypocenters located by all seismic stations (gray circles) and those by all but OBS stations (red circles). Triangles indicate positions of seismic stations for hypocenter determination. Translucent yellow area indicates that hypocenters had errors of several kilometers. The white lines indicate prefecture borders, and the bold black lines indicate the active faults.

cles). Regardless of the station arrangement, the epicenters are almost the same and differences are less than 1 km. However, differences in the focal depths are large. The yellow area of Figs. 4(a) and (b) shows where the hypocentral depth difference is more than about 1 km. When using only permanent stations, hypocenters from $X = -20$ km to $X = 6$ km that were shallower than 9 km, appeared deeper or shallower than when using all stations, with a maximum difference of about 5 km. Also, when using all but OBS stations, hypocenters from $X = -20$ km to $X = -15$ km that were shallower than 5 km appeared deeper than when using all stations, with a maximum difference of about 3 km. From this we can see that a hypocenter shallower than 9 km, which does not have a seismic station above it, can have an error of up to a 5 km in its depth assignment, even if we calculate hypocenters using reasonable structure and station correction values. However, events deeper than 9 km or near a station are well located regardless of the station distribution (i.e. except the yellow area of Fig. 4).

3.2 Hypocenter distribution and focal mechanisms

Figure 5 shows the distribution of the relocated hypocenters and the focal mechanism solutions for the major events. The aftershocks occurred beneath the Genkai-nada Sea, extending for about 25 km in a NW-SE direction, and they were in the range of 1–16 km deep. The aftershock distribution is deeper at the central part, while it is shallower at the margins (Fig. 5(b)). The mainshock occurred in the northwesterly central part of the aftershock region, at a depth of 9.5 km. The focal mechanism solution of the mainshock is strike-slip with a tension axis of N23°W–S23°E. From the above facts, we can infer that the source fault of the mainshock was left-lateral strike-slip.

From the aftershock distribution, we can recognize four main groups (Fig. 5). Group I extends from $X = -21$ km to $X = -15$ km in the direction of N45°W–S45°E with a dip of 90°(the thick translucent purple line shown in Figs. 6(i) and (ii)). Its shape is approximately linear, and there is a branch in the orthogonal direction. Group II, which includes the mainshock, extends from $X = -15$ km to $X = 3$ km in the direction of about N60°W–S60°E (the thick translucent yellow line shown in Figs. 6(i) and (iii)-(v)). There are two fault planes bordering on a depth of about 10 km, i.e. nearly at the depth of the mainshock. Concerning the dip angle, while it is a vertical plane in the depth range of 1 to 10 km, it is inclined at 80° downward to N30°E in the depth range of 10 to 16 km. Also, concerning the strike, there is about a 10-degree difference between two planes (Fig. 7). The fault plane of the deeper section is in good agreement with that of the focal mechanism solution of the mainshock (Fig. 7). Group III extends from $X = 3$ km to $X = 12$ km and includes the largest aftershock (Mj=5.8), which occurred just beneath Shikanoshima Island on April 20 at a depth of 11.5 km. The earthquakes lie on a plane which extends N45°W–S45°E and is inclined at 80°downward to S45°E, with a depth range of 8–14 km (the thick translucent blue line shown in Figs. 6(i) and

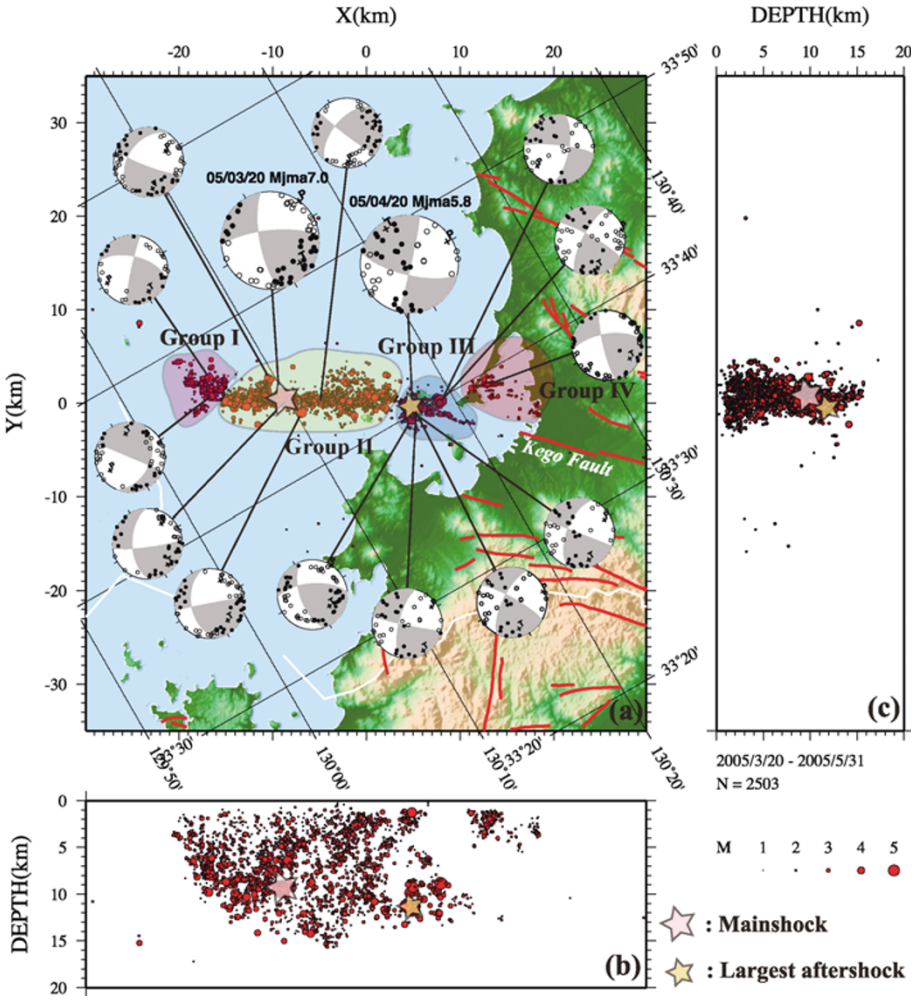

Fig. 5. Distribution of the relocated hypocenters from March 20 to May 31, 2005, and the focal mechanisms of the major events calculated from polarity data of *P*-wave first motions using the method of Kobayashi and Nakanishi (1994). (a) Epicenter distribution and the focal mechanisms of major events. Note that the map is rotated counterclockwise by 30 degrees so that the X-axis is parallel to the aftershock distribution. The red lines indicate active faults. The translucent purple, yellow, blue and red areas indicate the extent of each group described in the text. The focal mechanism diagrams are shown, using an equal-area projection on the lower hemisphere. Black and white circles show "push" and "pull" of *P*-wave first motions, respectively. (b) Depth distribution projected in the Y direction. (c) Depth distribution projected in the X direction.

Fig. 6(vi)). From this result and the mechanism solution of the largest aftershock (Fig. 7), its fault plane appears to be left-lateral strike-slip. The active Kego fault lies on an extension of this fault plane (The Research Group for Active Faults of Japan, 1991). Group IV extends about 5 km east of Group III, and the hypocenter depths are shallower than 3 km. The thick translucent red line (Figs. 7(i) and (vii)) indicates the estimated fault plane. The strike of this plane is the same as that of Group II.

4. Discussion

Concerning epicenter positions, when *P* and *S* arrivals were picked using more than 16 permanent stations, no matter what method was used, the results were almost the same. The differences are less than 1 km. But concerning focal depths, if we did not have arrivals at seismic stations above the focal region, some hypocenters appeared deeper or shallower by up to 5 km compared with their relocated values using all the stations. Therefore, if we want to obtain precise hypocenter positions, especially depth, we must get data from seismic stations above the focal regions.

We estimated four aftershock groups. Groups I to III are contiguous, but the strike of the fault plane changes on the boundary. This shows that the crustal structure is inhomogeneous at the I–II and II–III boundaries. The recent acoustic profiling at Hakata Bay (Okamura *et al.*, 2006) shows that the Kego fault extends to the Group III area. Thus we speculate that some of the hypocenters of Group III (the translucent blue line in Figs. 6 (i) and (vi)) are on the Kego fault plane and that is why the direction of hypocenter distribution differs between Groups II and III.

In Group II, which includes the mainshock, we estimated two fault planes (the thick translucent yellow lines of Fig. 6) bordering on the depth of the mainshock. There are 10-degree differences both of the strike and the dip angles between lower and upper planes. The fault-plane solution for the mainshock inferred from the polarity of *P*-wave first motions is consistent with the deeper plane (Fig. 7). On the other hand, the moment tensor solution of the mainshock, inferred from the waveform data of the broadband seismometer network (Matsumoto, T. *et al.*, 2006), is consistent with the upper plane. These facts imply the following. The

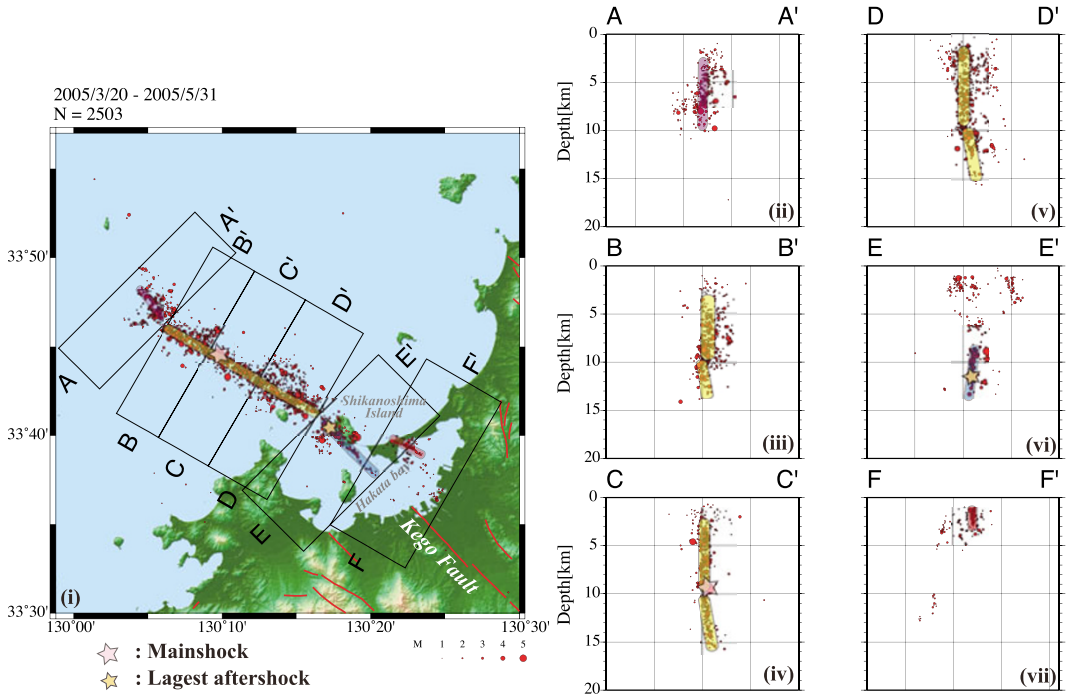

Fig. 6. Depth distribution of the relocated hypocenters in the rectangles of (ii) A-A′, (iii) B-B′, (iv) C-C′, (v) D-D′, (vi) E-E′ and (vii) F-F′ shown in (i). The thick translucent purple, yellow, blue and red lines indicate the estimated fault planes.

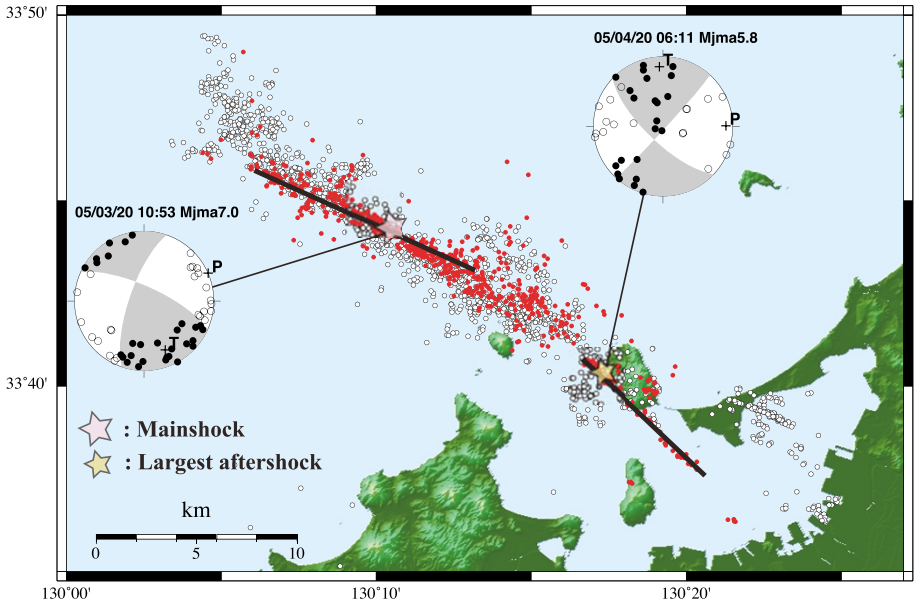

Fig. 7. Epicenter distribution and the focal mechanisms of the mainshock and the largest aftershock. Red and white circles denote epicenters deeper and shallower than the depth of the mainshock (depth=9.5 km), respectively. Two black solid lines indicate the strikes from the focal mechanism solutions of the mainshock and the largest aftershock.

rupture started from the hypocenter of the mainshock and propagated downward and then the lower plane ruptured. Next, the upper plane ruptured. The fact that the moment was released more in the upper plane rather than in the deeper plane (Asano and Iwata, 2006) supports the fact that the fault-plane solution of the moment tensor is almost the same with the upper plane.

There is a gap in the distribution of aftershocks southeast of the mainshock (Fig. 5(b)). According to the slip distribution obtained by waveform inversion (e.g. Asano and Iwata, 2006; Horikawa, 2006), the slip in this area is large. Perhaps most of the accumulated stress was released when the mainshock occurred, so the aftershock activity was very low.

Roughly speaking, the aftershock distribution extends in the direction of NW-SE in vertical planes, and also the strikes of active faults in the Fukuoka prefecture (The Research Group for Active Faults of Japan, 1991) lie in almost the same direction as the aftershock distribution. In addition, Quaternary crustal movement in the northern part of

Kyushu was not active (Machida *et al.*, 2001). Therefore we surmise that the stress field in the northern part of Kyushu was almost the same during the Quaternary.

5. Conclusions

We deployed temporary seismic stations just above the aftershock area, combined data from the temporary stations and from permanent stations around the aftershock area, and relocated aftershocks using the JHD technique. Then we obtained precise hypocenter distributions, especially for depth. The relocated hypocenter parameters can be downloaded from **http://www.sevo.kyushu-u.ac.jp/2005-GENKAI/**.

The mainshock occurred in the northwesterly central part of the aftershock region (Group II) at a depth of 9.5 km. From its focal mechanisms and the aftershock distribution, the mainshock source fault was left-lateral strike-slip. The largest aftershock was in the southeast part of the aftershock region (Group III) at a depth of 11.5 km. From its focal mechanisms and the aftershock distribution, the source fault of the largest aftershock was also left-lateral strike-slip.

The earthquakes occurred in a depth range of 1–16 km, with the aftershock distribution deeper at the center and shallower at the margins. We found that the aftershocks could be divided into four groups. The strikes of Groups I and III are different from that of Group II. In Group II, we estimated two fault planes bordering on the depth of the mainshock. There are 10-degree differences both of the strike and the dip angles between lower and upper planes. From the aftershock distribution and the focal mechanisms, the rupture first propagated downward, then propagated upward.

Acknowledgments. We would like to express our gratitude to Drs. N. Kame and A. Watanabe, Messrs. M. Tahara, M. Saito, and Ms. M. Hori for their on-board help with OBS observations. The work of the officers and crews of the M/V *Fujisan-maru*, and the P/V *Genkai* is appreciated. Fukuoka Federation of Fisheries Cooperative Associations, fisheries cooperatives of Fukuoka Prefecture, Fukuoka Fishers and Marine Technology Research Center, and Mr. I. Ooshiro of MEXT cooperated with the OBS observations. We also thank Ms. H. Katayama for her help in picking up arrival times. We used seismic data from Fukuoka City, JMA and NIED. Comments by reviewers (Dr. S. Ross and Dr. Y. Ito) helped us improve the manuscript. Most of the figures were created using GMT (Wessel and Smith, 1995).

References

Asano, K. and T. Iwata, Source process and near-source ground motions of the 2005 west Off Fukuoka Prefecture earthquake, *Earth Planets Space*, **58**, 93–98, 2006.

Geographical Survey Institute, *Horizontal strain in Japan 1985–1883*, 133 pp, ASSOCIATION FOR THE DEVELOPMENT OF EARTHQUAKE PREDICTION, 1987 (in Japanese).

Hirata, N. and M. Matsu'ura, Maximum-likelihood estimation of hypocenter with origin time eliminated using nonlinear inversion technique, *Phys. Earth Planet. Inter.*, **47**, 50–61, 1987.

Hori, M., S. Matsumoto, K. Uehira, T. Okada, T. Yamada, Y. Iio, M. Shinohara, H. Miyamachi, H. Takahashi, K. Nakahigashi, A. Watanabe, T. Matsushima, N. Matsuwo, T. Kanazawa, and H. Shimizu, 3D seismic velocity structure in and around the focal area of the 2005 west Off Fukuoka prefecture earthquake by double-difference tomography, *Earth Planets Space*, **58**, this issue, 1621–1626, 2006.

Horikawa, H., Rupture Process of the 2005 West Off Fukuoka Prefecture, Japan, earthquake, *Earth Planets Space*, **58**, 87–92, 2006.

Iio, Y., H. Katao, T. Ueno, B. Enescu, N. Hirano, T. Okada, N. Uchida, S. Matsumoto, T. Matsushima, K. Uehira, and H. Shimizu, Spatial distribution of static stress drops for aftershocks of the 2005 West Off Fukuoka Prefecture earthquake, *Earth Planets Space*, **58**, this issue, 1611–1615, 2006.

Kissling, E., W. L. Ellsworth, D. Eberhart-Phillips, and U. Kradolfer, Initial reference models in local earthquake tomography, *J. Geophys. Res.*, **99**, 19635–19646, 1994.

Kobayashi, R. and I. Nakanishi, Application of genetic algorithms to focal mechanism determination, *Geophys. Res. Lett.*, **21**, 729–732, 1994.

Machida, H., Y. Ota, T. Kawana, H. Moriwaki, and S. Nagaoka, *Regional Geomorphology of the Japanese Islans, vol. 7 Geomorphology of Kyushu and the Ryukyus*, 355 pp, University of Tokyo Press, 2001 (in Japanese).

Matsumoto, S., A. Watanabe, T. Matsushima, H. Miyamachi, and S. Hirano, Imaging *S*-wave scatterer distribution in southeast part of the focal area of the 2005 West Off Fukuoka Prefecture Earthquake (M_{JMA}7.0) by dense seismic array, *Earth Planets Space*, **58**, this issue, 1627–1632, 2006.

Matsumoto, T., Y. Ito, H. Matsubayashi, and S. Sekiguchi, Spatial distribution of F-net moment tensors of the 2005 West Off Fukuoka Prefecture Earthquake determined by the extended method of the NIED F-Net routine, *Earth Planets Space*, **58**, 63–67, 2006.

Nakao, S., H. Takahashi, T. Matsushima, Y. Kohno, and M. Ichiyanagi, Postseismic deformation following the 2005 West Off Fukuoka Prefecture Earthquake (M7.0) derived by GPS observation, *Earth Planets Space*, **58**, this issue, 1617–1620, 2006.

Okamura, M., H. Matsuoka, K. Shimazaki, N. Chida, T. Nakata, and K. Hirata, Paleoseismicity on the extension of the Kego Fault in Hakata Bay, *Rep. Coord. Comm. Earthq. Pred.*, **75**, 555–559, 2006 (in Japanese).

Sagiya, T., S. Miyazaki, and T. Tada, Continuous GPS Array and Present-day Crustal Deformation of Japan, *PAGEOPH*, **157**, 2303–2322, 2000.

Shimizu, H., H. Takahashi, T. Okada, T. Kanazawa, Y. Iio, H. Miyamachi, T. Matsushima, M. Ichiyanagi, N. Uchida, T. Iwasaki, H. Katao, K. Goto, S. Matsumoto, N. Hirata, S. Nakao, K. Uehira, M. Shinohara, H. Yakiwara, N. Kame, T. Urabe, N. Matsuwo, T. Yamada, A. Watanabe, K. Nakahigashi, B. Enescu, K. Uchida, S. Hashimoto, S. Hirano, T. Yagi, Y. Kohno, T. Ueno, M. Saito, and M. Hori, Aftershock seismicity and fault structure of the 2005 West Off Fukuoka Prefecture Earthquake (M_{JMA}7.0) derived from urgent joint observations, *Earth Planets Space*, **58**, this issue, 1599–1604, 2006.

The Research Group for Active Faults of Japan, *Active Faults in Japan* (revised edition), 448 pp, University of Tokyo Press, 1991 (in Japanese).

Uehira, K. and H. Shimizu, Surprise and teachings from the 2005 West off Fukuoka Prefecture Earthquake, *Science Journal KAGAKU*, **75**, 795–797, 2005 (in Japanese).

Urabe, T. and S. Tsukada, A workstation-assisted processing system for waveform data from microearthquake networks, *Abstracts of Spring Meeting of Seismological Society of Japan*, p. 70, 1991 (in Japanese).

Watanabe, A., S. Matsumoto, T. Matsushima, K. Uehira, N. Matsuwo, and H. Shimizu, Shear wave polarization anisotropy in and around the focal region of the 2005 West Off Fukuoka Prefecture Earthquake, *Earth Planets Space*, **58**, this issue, 1633–1636, 2006.

Watanabe, H., Determination of earthquake magnitude at regional distance in and near Japan, *Zisin 2*, **24**, 189–200, 1971 (in Japanese with English abstract).

Wessel, P. and W. H. F. Smith, New version of generic mapping tools released, *EOS Trans. AGU*, **76**, 329–336, 1995.

K. Uehira (e-mail: uehira@sevo.kyushu-u.ac.jp), T. Yamada, M. Shinohara, K. Nakahigashi, H. Miyamachi, Y. Iio, T. Okada, H. Takahashi, N. Matsuwo, K. Uchida, T. Kanazawa, and H. Shimizu